RPT-O-G0021

Response of the Primary Mirror to Support System Errors

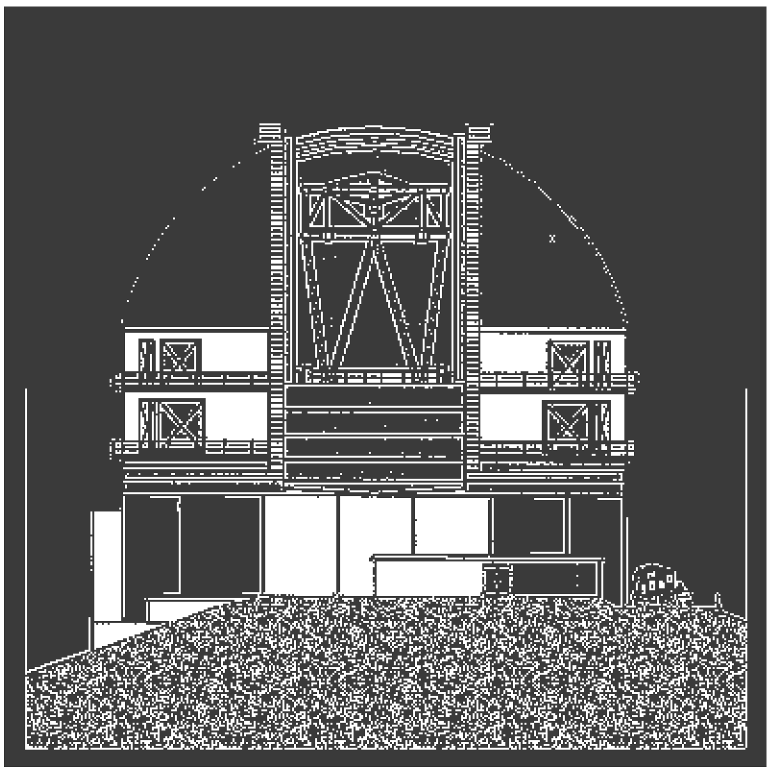

Myung K. Cho
Opto-structural Engineer

John L. Roberts
Opto-mechanical Engineer

November 1993

GEMINI PROJECT OFFICE 950 N. Cherry Ave. Tucson, Arizona 85719
Phone: (602) 325-9329 Fax: (602) 322-8590

Table of Contents

SUMMARY

This report analyzes the sensitivity of the primary mirror surface, and resulting optical performance effects, to possible errors in the Gemini primary mirror axial and lateral support systems. The results of these analyses are used to establish limits for these errors. Tolerances for primary mirror cell subassemblies, subsystems and piece parts will be developed from the results.

The analytical framework of this tolerance analysis is first discussed, and a number of specific error cases defined. These error cases represent the types of errors that may result from errors or tolerances in the individual components of the support systems and from specific events that produce systematic errors, such as differential thermal expansion between the mirror and the mirror cell.

Unit load cases were analyzed using finite element techniques. Deformations of the mirror surface were calculated. These deformations were applied to the primary mirror surface, in the telescope model of the optical analysis ray trace program, for each unit load case and the effects on telescope performance were evaluated. The results on the optical figure and optical performance of each case are discussed in turn. The analysis techniques and results for the unit load cases are presented in Section 2.

The unit load cases are combined into nine cases or categories of errors for the error budget. The error budget is expressed in terms of allowable errors for the mechanical parts of the primary mirror support system. The hardware will be designed to meet these requirements. Image quality degradation and maximum allowable errors for error budget items are itemized in Section 3. The total effect on image quality and plate scale change are tabulated below along with the requirements.

	encircled energy degradation, arcsecond				plate scale change	
	zenith		75°		ppm	
	50%	85%	50%	85%	zenith	75°
requirement	0.010	0.022	0.079	0.196	40	40
result, rss *	0.009	0.018	0.064	0.101	32	35

* total of all items in the error budget, results are itemized in section 3

Additional allowance remains for any change in performance of the primary mirror support systems from other as yet unforeseen errors. At zenith pointing the remaining allowance for 50% encircled energy is .0049 arcsecond and .0133 arcsecond for 85%. At a zenith angle of 75°, the remaining allowance is .0456 arcsecond for 50% and .1679 arcsecond for 85%.

The overall conclusion of this analysis is that the allowable tolerances on the support system are clearly achievable. All the error cases analyzed could be corrected by the low order active optics loop giving residual errors on the primary mirror surface that were well within the 2.2 µm error budget.

The sensitivity to pressure errors in the hydraulic zones were higher than anticipated and the design effort will focus on controlling this factor. Other component and subsystem tolerances were well within reasonable engineering margins. An example is the maximum allowable random force error. The requirement for repeatability for the axial actuators was found to be 2.0 Newtons. This is a maximum error of 0.2% of the nominal load. Load cells are available that better this amount by almost an order of magnitude.

Section 1
INTRODUCTION

1.1 Purpose of Analyses

Fabrication, assembly, alignment and calibration errors in the primary mirror support system could result in distortions of the mirror. Other events such as changing gravity orientation (zenith angle), distortions of the mirror cell or rigid body movements of the mirror would produce patterns of errors. These analyses were undertaken to establish mechanical tolerances for these errors.

Maximum values for various effects of the errors, as they are applied to the mirror, are established. The tolerances developed in these analyses apply only to the mechanical subsystems. Tolerances for individual piece parts or subassemblies are not in this report. A separate error budget applies to the control system and other sources of errors.

1.2 Types of Errors

The error cases analyzed are combinations of errors for each portion of the mirror support system. The combinations of errors may be random in nature or may be systematic patterns of errors resulting from specific events. The combinations of errors fall into four general categories. The first three categories are concerned with the support of the mirror in the axial direction. The first category contains combinations of errors in the axial supports. The second is errors in the air support system. The third category is concerned with the six zone defining system. The fourth category is the lateral support system.

At each support actuator location four different errors may exist. The errors may be in the magnitude of the force, the location the force is applied at, force components in directions other than the intended direction or unintended moments exerted on the mirror. These errors may be present in the axial support system and in the lateral support system.

The air support system is designed to furnish much of the support for the mirror in the axial direction. It does this by maintaining a slight positive gauge pressure in the space between the mirror and the mirror cell. The system is designed so the axial actuators exert a force equal to twenty percent of the mirror's weight. In order to maintain the air at the appropriate pressure, seals are incorporated near the outer edge and near the central hole of the mirror. These seals will also exert forces on the mirror.

A passive hydraulic system is used in the axial support system. In low wind conditions it could be used as three zones making it statically determinate. When wind velocity rises beyond a certain level, valves within each zone could be closed separating each into two zones. This turns the hydraulic system into a six zone defining system. Errors in the volume of fluid, or pressure in each zone, could result in distortions of the mirror surface.

1.3 Sources of Errors

Potential errors are associated with each portion of the mirror support system. Components of each subsystem will have errors that are consistent with their configuration.

1.3.1 Axial Supports

The axial supports consist of a passive hydraulic system and an active mechanical system. Errors may result from:

- fabrication and assembly tolerances in the passive and active components
- load cell calibration tolerances, finite resolution and non-linearities
- actuator installation and alignment tolerances
- non-repeatability in reinstallation of the mirror after recoating

Other errors that are associated with the axial actuators may be the result of differential thermal expansion between the mirror and the mirror cell or shifting of the mirror relative to the mirror cell. At the point of attachment to the mirror, a flexure is used to transmit the force to the mirror. With any lateral shift the flexure will exert a moment on the mirror. It will also exert a lateral force resisting any shift in mirror position.

1.3.2 Air Support System

The space between the mirror and the mirror cell is sealed to maintain the air between them at a slight positive gauge pressure. The system is designed for the axial supports to carry a nominal force of twenty percent of the mirror's weight. Deviation from the nominal air pressure may cause a small amount of print through of the axial actuators to the mirror's optical surface.

In order to maintain the pressure difference, seals are used near the outer and inner edges of the mirror. These seals may exert forces that are higher or lower than planned. As the seal inflates or the mirror cell expands, a radial force may be applied to the mirror. Any shift or tilt of the mirror will cause forces on the mirror to depart from the nominal value. Any bending of the mirror cell will also cause forces between the seals and the mirror to deviate from nominal.

1.3.3 Six Zone Defining System

In low wind conditions the mirror may be supported by a three zone hydraulic whiffle-tree. Each of the three zones incorporates a valve that connects or isolates halves of the zone. When conditions dictate, the valves may be either throttled or closed. With the valves throttled the system becomes a damped three zone system. When the valves are closed it becomes a six zone defining system providing superior resistance to wind buffeting. A complete description of the system function is given in the report *The Distributed Defining System for the Primary Mirrors*. Errors in the volume of fluid in the six zones could cause a distortion of the mirror optical surface.

1.3.4 Lateral Support System

The lateral support actuators are similar in design to the axial actuators. They are susceptible to the same errors as the axial actuators.

1.4 Primary Mirror Axes

References are made to different directions in this report. The Z axis is the optical axis of the primary mirror. The X axis is the elevation axis of the telescope. The Y direction is orthogonal to the X and Z axes and is vertical with the mirror in the horizon pointing orientation. The axial direction is along the Z direction. The normal direction is perpendicular to the mirror optical surface and therefore has components in the X, Y and Z directions. The axial actuators act in the normal direction. Directions orthogonal to the normal direction also have components in the X, Y and Z directions.

1.5 Related Material

The design philosophy guiding the development of the primary mirror assembly is discussed in the report *Conceptual Design of the Primary Mirror Cell Assembly*. The defining system for the primary mirror assembly is discussed in the report *Primary Mirror Forces from a Distributed Hydraulic "Axial" Support System* and *The Distributed Defining System for the Primary Mirrors*. Optimization of the support system is detailed in the report

Optimization of Support Point Locations and Force Levels of the Primary Mirror Support System. These reports should be consulted for more in depth discussion of the primary mirror support system.

Section 2
ANALYSIS

2.1 Errors Analyzed

The errors analyzed are combinations of errors at each point that the support systems touch the mirror. The combinations may be random in nature or patterns arising from specific events. Each combination considered will be discussed along with the results of the analyses.

Patterns of errors are combinations of discrete errors. A discrete error is one particular error applied at one location. The patterns of errors may be random or systematic in nature. Some of the combinations are the result of specific events such as differential thermal expansion between the mirror and the mirror cell. Other combinations are random such as random force magnitude errors resulting from errors in the actuators, installation and alignment of the actuators and the finite ability to sense and adjust the magnitudes of the forces they apply. The combinations that comprise the error budget are discussed in section 3. They are composed of the combinations analyzed here.

The axial and lateral support optimizations were performed in the zenith pointing orientation and then analyzed at other zenith angles. The analyses in this section were performed without regard to zenith angle. Appropriate side loads and moments are scaled and combined with these analyses in the error budget section to take into account telescope elevation orientation.

The results of the analyses of the unit load cases are given in this section. Unit loads were assumed for each effect prior to performing the analyses. The unit loads may, therefore, be different from the values established in the error budget. They are chosen to represent reasonable values for effects or to evaluate the mirror's sensitivity to some effects. Contour plots of the mirror surface deformations arising from the unit load cases are presented. Due to the wide range of surface deformations, particularly before and after correction with the active optics system, no single contour interval could represent all of the deformations. This range of contour intervals used must be noted in interpreting the plots.

2.2 General Description of Analysis Methods

2.2.1 Error Generation

2.2.1.1 Discrete Errors

The actuators, axial and lateral, were analyzed as discrete error sources. The effects of errors in force magnitude, force location, force direction and moments applied to the mirror by the mounting features were analyzed. The errors were introduced individually at each support location. The resulting deformation of the mirror surface was evaluated for each discrete error. These discrete errors and their effects on the mirror surface are then combined by superposition to form the error combinations analyzed.

The air pressure fluctuations were analyzed by increasing and decreasing the weight supported by the air pressure support system. This changes the forces applied by the axial actuators. The resulting print through of the actuators to the mirror surface was then obtained using nominal axial actuator locations.

The air pressure seals were not analyzed with random combinations of errors. The seals are continuous entities and the errors in forces applied by them must be consistent with their nature as continuous entities. They were instead analyzed using patterns of errors at their locations, either a constant force per unit length or a force component that is a function of angular position.

2.2.1.2 Error Combinations

Error combination patterns were generated randomly or systematically depending on the error considered. Gaussian distributions were used for the random combinations. A value for three standard deviations was chosen to represent the accumulation of mechanical tolerances at the piece part or subassembly level. They resulted in random magnitudes in random patterns. The unit cases were then scaled to appropriate levels for use in the error budget.

Systematic errors are definite patterns of errors in the support forces. They are the result of a specific event such as thermal expansion differences between the mirror and the mirror cell. They were analyzed by exerting unit force cases and moments at the appropriate locations in a predetermined pattern of magnitudes and directions. The patterns are derived from the definition of the error considered. Systematic error combinations were analyzed with unit loads and then scaled to the appropriate values for the error budget, based on properties of the support system components. An example would be to use the unit load for mirror decenter in the Y direction and the stiffness of the flexures in the axial supports to obtain a maximum allowable value for decenter.

The errors and the resulting effects are linear and independent. They may, therefore, be added in quadrature. This allows them to be analyzed independently and the total effect on telescope performance to be the quadrature sum of the individual effects.

2.2.2 Finite Element Analysis

2.2.2.1 Finite Element Model (FEM)

For these analyses a full model of the mirror was constructed. This is necessary due to the non-symmetric nature of the applied forces and moments at individual actuator locations. The defining system was simulated by using nine multiple point constraints (MPC), to represent the nine hydraulic zones in the defining system, six axial and three lateral. The sums of the axial forces along the three axes and the moments about each of the lateral axes are constrained to equal zero.

The model consists of 2304 elements and 2304 nodes. The model uses plate bending elements. The actuator loads are applied at nodes in the mid-plane of the model.

The MPC's do not allow the actuators within a zone of the defining system to act independently of the other actuators within that zone. The actuators within each zone contain a fixed amount of hydraulic fluid, therefore the net displacement of the actuators in a zone must be a constant determined by the volume of fluid and the mechanical properties of the mirror cell and the actuators. The pressure of the fluid within a zone must remain constant within that zone. The force exerted by the passive hydraulic portion of the actuator is determined only by the pressure and the area of the hydraulic piston.

The loads are applied at a total of 336 nodes. They correspond to the actuator locations and at each node over the air pressure seals. At each of these nodes three force components and two moment components may be applied.

For any force applied at other than the nominal location or in a direction other than normal to the surface, the force must be resolved to the nominal location with forces and moments. This is necessitated as forces and moments may only be applied at nodes in the FEM. Forces orthogonal to the normal force, applied at the back surface of the mirror, must be simulated by a moment whose moment arm is equal to one half the mirror thickness, plus force components in three directions. Forces normal to the mirror surface but applied at other than nominal location are simulated with a force equal and a moment applied at the nominal position. The force is equal in magnitude to the actual force and the moment is equal to the product of the magnitude of the force and a moment arm equal to the displacement of the force from the nominal position.

The geometry of the FEM is shown in Figure 2-1. The six zones of the axial defining system are also shown. The X axis shown is the direction of the elevation axis of the telescope. At horizon pointing the Y axis is oriented vertically up.

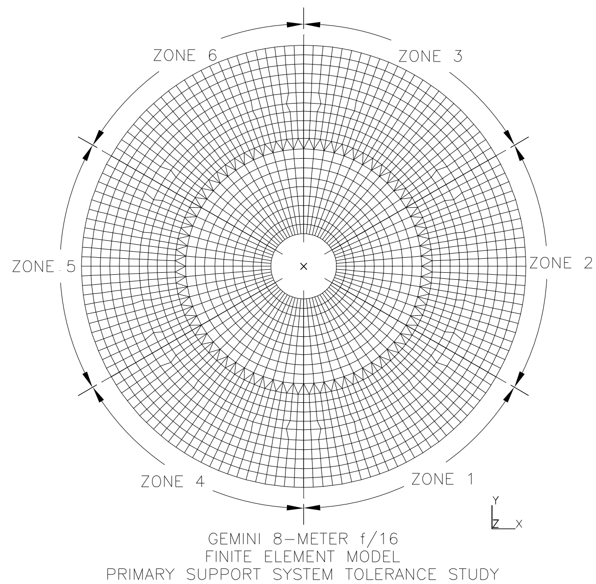

Figure 2-1: Finite Element Model

2.2.2.2 Discrete Errors

The discrete errors were analyzed by applying unit loads at the actuator locations one at a time. There are a total of 1680 unit cases. At each of the 336 nodes where loads were applied, three unit forces and two unit moments were applied in turn. The forces and moments correspond to the five degrees of freedom at each of those nodes. The deformation of the mirror was found for each case. These deformations were used to construct the influence matrix for the mirror.

2.2.2.3 Influence Matrix

The effects of each unit load were used to construct a global deformation matrix. Each combination of errors in the support system is represented by a vector of forces and moments for the points at which the support systems touch the mirror. The Influence matrix is multiplied by this vector. The product is the deformation at each node on the mirror's surface. The total deformation of the mirror optical surface is thus obtained for evaluation of its effect on image quality and plate scale.

The influence matrix has 2304 rows and 1680 columns. The number of rows correspond to the number of nodes at which the deformations are calculated. The columns correspond to the unit loads described in 2.2.2.2. When the influence matrix is multiplied by a vector representing a load case, the deformation at each of the nodes is found.

2.2.2.4 Error Combinations

The error combinations were generated consistent with their definitions, either random or systematic. Each case was represented by a vector of the normal forces, orthogonal force components and moments. The influence matrix was then multiplied by these vectors to determine the total deformation of the mirror surface for each combination.

The effects of each error combination are analyzed by using unit load cases. Magnitudes of the errors used were chosen as being representative of manufacturing errors or for computational ease. The errors are independent and sufficiently small that the resulting effects are linear and may be scaled up or down by reasonable amounts.

After the surface deformation is found, correction with the active optics system is simulated. The forces exerted by the axial actuators are used to optimize the mirror surface. One of the unit load cases represents random force magnitude errors for all of the support actuators. This simulates the resolution to which the active optics system is able to set the forces at each actuator. This case is not corrected. The other cases do not consider the resolution of the actuators. The correction may also be scaled with the unit load cases.

2.2.3 Optical Analysis

2.2.3.1 General Procedure

All analyses were performed using the f/16 telescope model at a wavelength of 2.2μm at the on axis field position. Calculated deformations were analyzed for image quality degradation using the Code V™ optical analysis package produced by Optical Research Associates in Pasadena, California. Interferogram files were generated from the results of the finite element analyses. These files are in a grid format, a 512 by 512 grid was used.

Prior to analysis, piston, tilt and focus were removed from the deformations. The focus removed was used to calculate the change in plate scale. The deformations were then applied to the primary mirror in the Code V™ model. Image quality was then evaluated. The results are given in Section 2.3.

2.2.3.2 Image Quality Analysis

Encircled energy was calculated using the diffraction based point spread function, PSF, option of Code V™. The results were compared to the telescope with zero deformation by quadrature subtraction. All image quality calculations were performed for the on-axis field position. An improvement in the accuracy of encircled energy is possible by scaling the deformations to a significant level and then scaling the quadrature difference back with the same scaling factor. Correlation was found to be good if the surface deformations are scaled up to a surface of 40 nm-rms. The quadrature difference was calculated for this surface deformation and then scaled back by the same factor used to scale the deformations up. This technique was found to give conservative results.

2.2.3.3 Plate Scale Change

Plate scale changes were evaluated using the amount of focus aberration present in the deformations of the finite element analysis. Ray trace analysis results show a plate scale change of one part in one million for a peak to valley spherical aberration of the primary mirror of 159.9 nm. This analysis assumed focus corrected by axial movement of the secondary mirror.

2.3 Detailed Description of the Analyses and Results

The unit load cases are described here. Values for the unit loads were chosen prior to establishing the error budget and may, therefore, be different from those values in a number of cases. Some of the load combinations here appear in more than one error budget case. This is because the unit load cases are of particular effects regardless of the cause. For example, forces in the Y direction at the axial actuator support points may be used to evaluate mirror decenter in the Y direction or the effect of the weight of the axial support pads in the horizon pointing orientation. Both apply a force in the same orthogonal direction, but of different magnitudes. The unit loads are scaled for the particular error budget item and combined as appropriate.

2.3.1 Random Combination of Normal Forces at Axial and Lateral Support Locations

This combination represents the resolution with which the active optics system can set the loads at the individual actuators. Therefore, the normal forces were not adjusted to optimize the mirror surface. Amplitudes of the normal force errors were generated with a random number generator. This technique produces normal force errors in a random pattern with a Gaussian distribution. The three standard deviation force was set at 2.0 Newtons. Each axial actuator will support less than 400 Newtons of the mirror's weight. An error of 2.0 Newton represents an inaccuracy of 0.5%. Load cells are available that have non-repeatabilities of 0.02%. The magnitude of the forces used is conservative. The deformation that was produced by this pattern had a peak to valley deformation of 64 nm and an rms value of 10.5 nm. A contour plot of the deformation is shown in figure 2-2.

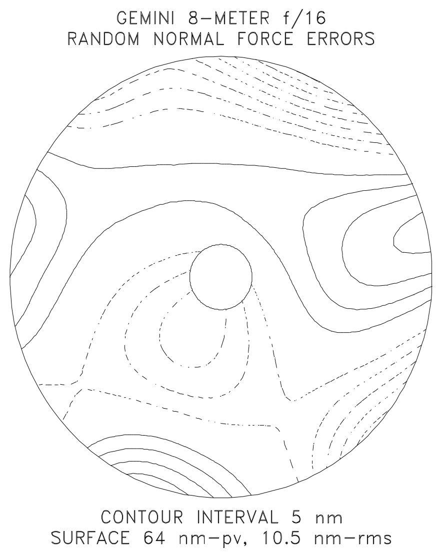

Figure 2-2: Typical Contour Plot from Random Normal Force Errors

The degradation in image quality for the f/16 telescope is .003640 arcsecond increase in the diameter encircling fifty percent of the energy and .010496 arcsecond increase for eighty five percent of the energy. The plate scale change calculated was .252 parts per million.

2.3.2 Random Combination of Position Errors at Axial Support Locations

This combination was analyzed in two parts. Random errors in position were analyzed in the radial direction and then in the tangential direction. Nominal forces were applied with errors in the radius of the actuators and then with errors in the position angle of the actuators. The errors are Gaussian distributions with a three standard deviation value of 2 mm. Positional accuracies of this magnitude are achievable in manufacturing. The effects on image quality were then combined in quadrature. The effects on plate scale were treated the same way.

The tangential errors produced a surface deformation of 51 nm peak to valley and 8.0 nm rms prior to correction and were then improved to .57 nm peak to valley and .066 nm rms with active optics. The radial errors induced surface errors of 41 nm peak to valley and 7.1 nm rms without correction by the active optics system. The surface was improved to .029 nm peak to valley and .0022 nm rms. In both directions the surface was improved by more than three orders of magnitude.

Contour plots of the surface deformations are shown in figures 2-3 and 2-4. The figures show the mirror surface before correction and after correction with the active optics system. In interpreting the figures, observe the difference in the contour intervals.

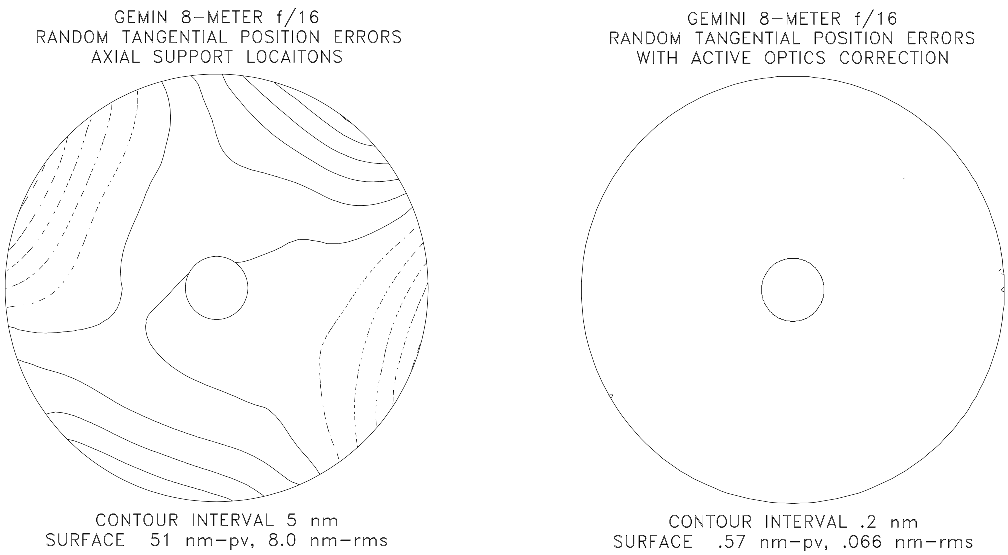

Figure 2-3: Effects of Random Tangential Position Errors

For the tangential position errors, the increase in the diameter for fifty percent encircled energy is 28.3×10^{-6} arcsecond. For 85 percent the increase is $.175\times10^{-3}$ arcsecond.

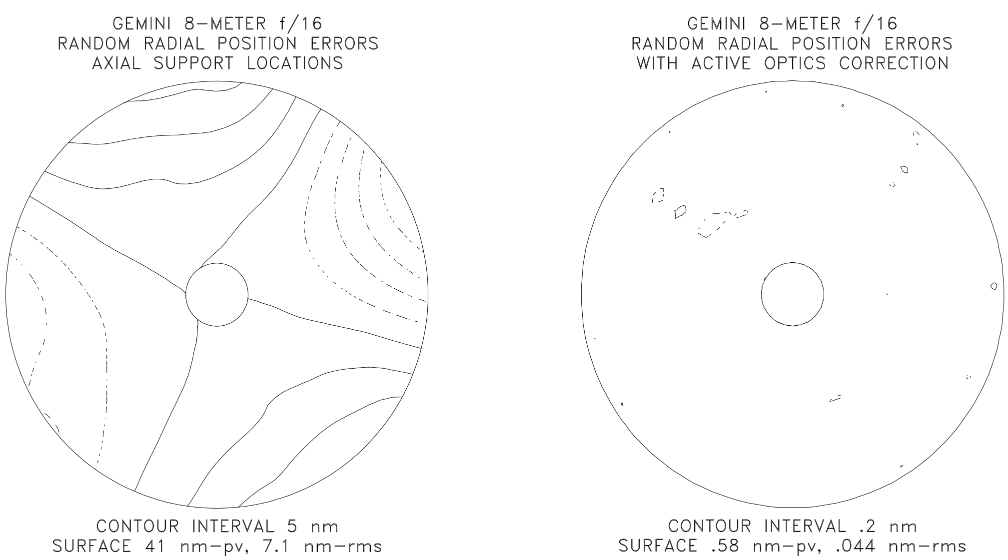

Figure 2-4: Effects of Random Radial Position Errors

The increase in the diameter for fifty percent encircled energy for the radial position errors is 16.3×10^{-6} arcsecond and 98.3×10^{-6} arcsecond for 85 percent. The combined increase in the diameter encircling fifty percent of the energy is 32.7×10^{-6} arcsecond for the two combinations. The total increase for 85 percent encircled energy is $.201\times10^{-3}$arcsecond. The plate scale change for the combined case is .039 parts per million.

2.3.3 Mirror Cell Expands, Axial Supports Exert Radial Forces as a Function of Radial Position

The radial positions at which the forces applied by the actuators were not changed. A radial force was applied at each support location proportional to each actuator's radial position. This simulates the effects of thermal expansion of the mirror cell when the supports are not given an opportunity to reseat themselves. This changes the direction at which the force is exerted by the axial actuators. The actuators are tilted inward. The unit load is 2 Newtons per meter of radius of support position. This simulates an expansion of 81.38 parts per million, or 81.38 µm per meter of radius. For the mirror cell made of steel and for a zero expansion of the ULE™, this would correspond to a change in temperature of 6°C. The expected overnight change in temperature is no more than 5°C. Prior to correction by the active optics system, the mirror surface had a figure of 12 nm peak to valley and 3.3 nm rms. With correction the surface was improved to .92 nm peak to valley and .122 nm rms. Contour plots of the uncorrected and corrected surface are shown in figure 2-5. In interpreting the contour plots note the difference in contour intervals.

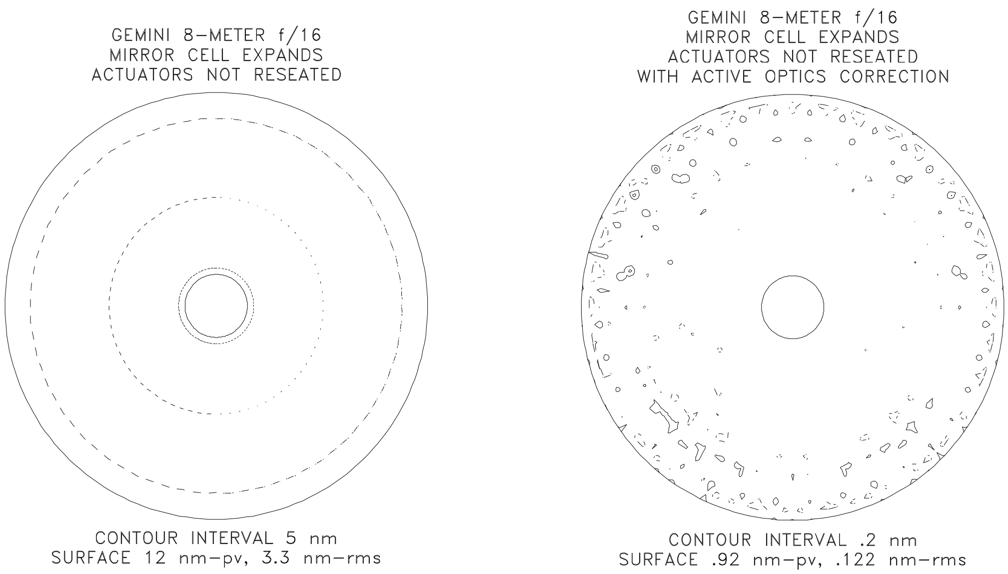

Figure 2-5: Mirror Cell Expands, Supports not Reseated

The effect on image quality of the corrected surface was evaluated. The increase in diameter for fifty percent encircled energy is 43.2×10^{-6} arcsecond. The increase for 85 percent encircled energy is $.249\times10^{-3}$ arcsecond. The plate scale change is 1.956 parts per million.

2.3.4 Random Pressure Errors in the Six Zones

A Gaussian distribution of pressure differences between the six zones was generated. The three standard deviation value for the distribution was .12 Newton per actuator. The six zone defining system is a hydraulic system. The system will be controlled by measuring and controlling the pressure differences between the zones. The amount of hydraulic fluid in each zone is regulated and the net axial position is determined by the volume of fluid in each zone and deflections of the mirror, the mirror cell and the actuators. No active optics correction was applied in this case because this case evaluates the allowable zoned pressure changes during the time between active optics updates. See report *The Distributed Defining System for the Primary Mirrors* for a complete description of the system's functioning.

The surface deformation produced was 79 nm peak to valley and 14.7 nm rms. A contour plot of the surface is shown in figure 2-6.

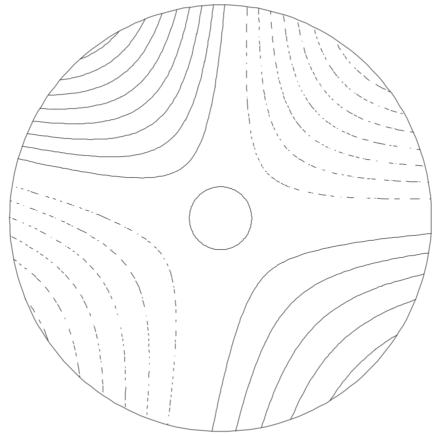

Figure 2-6: Effect of Random Pressure Errors in the Six Zone Defining System

The increase in the diameter encircling fifty percent of the energy is 6.67×10^{-3} arcsecond. The increase for 85 percent of the energy is 10.14×10^{-3} arcsecond. There is no change in plate scale from this combination.

2.3.5 Symmetrical Radial Force Errors at the Outer Air Seal

A radial force of four Newtons was applied at each node over the outer air pressure seal. There are 144 nodes to which the loads are applied. This translates into 22.56 Newtons per meter of circumference. This unit load case simulates the effect of differential thermal expansion between the mirror and the mirror cell, over-inflation of the seal or anything that would cause a radial mismatch between the mirror and the seal or mirror cell. This case is used to set the limits on those properties of the seal.

Prior to correction with the active optics system the surface deformation produced was 13.6 nm peak to valley and 4.0 nm rms. The surface was improved with the active optics system to .83 nm peak to valley and .119 nm rms. Contour plots of the surface prior to correction and after correction with the active optics system are in figure 2-7. In interpreting the plots note there is a difference between the contour intervals of the two plots.

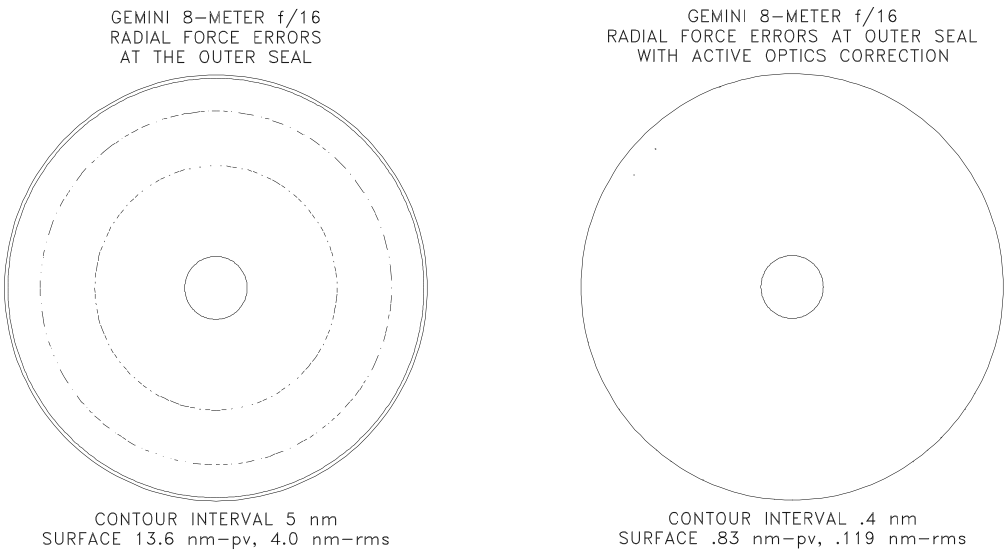

Figure 2-7: Effect of Radial Force Applied by the Outer Air Pressure Seal

The image quality degradation that resulted from the corrected surface was evaluated. The increase in the diameter encircling fifty percent of the energy is 37.6×10^{-6} arcsecond. For 85 percent encircled energy the increase is $.204\times10^{-3}$ arcsecond. The change in plate scale is 1.103 parts per million.

2.3.6 Mirror Cell Expands, Axial Supports Relocated Radially as a Function of Radial Position

The radial position of the actuators was increased 400 µm per meter of radius (400 parts per million). This would simulate a change in temperature of 29°C. A temperature change of this magnitude could exist between the environment at which the mirror is tested in the optics shop and the operating environment. The surface figure prior to any active optics correction is 7.8 nm peak to valley and 2.2 nm rms. After correction with the active optics system the surface figure is .82 nm peak to valley and .10 nm rms. Figure 2-8 shows the mirror surface prior to and after correction. Observe that there is a difference between the contour intervals in the two figures.

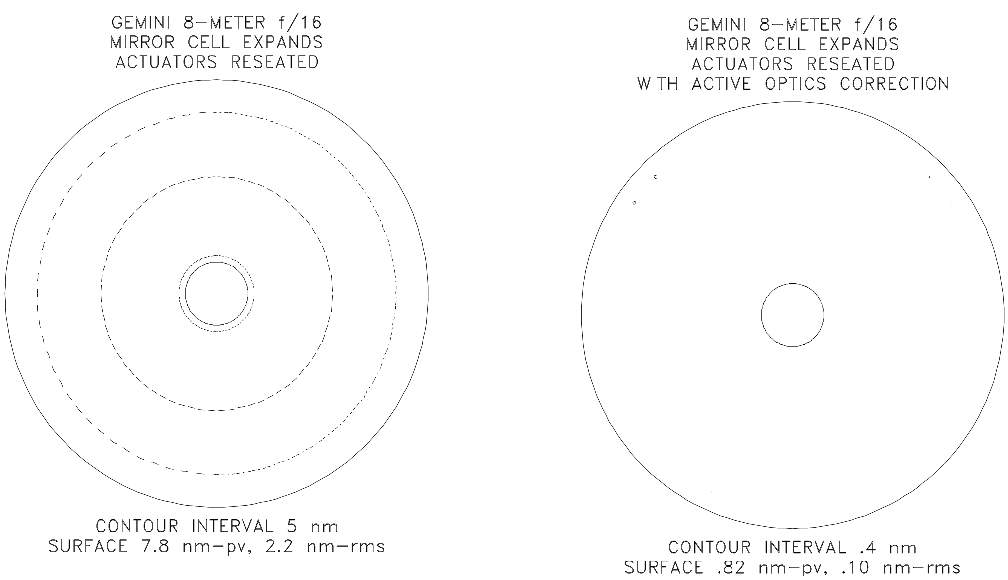

Figure 2-8: Effect of Mirror Thermal Expansion, Supports Reseated

Effects on image quality were evaluated. The increase in diameter for fifty percent encircled energy is 34.3×10^{-6} arcsecond. For 85 percent encircled energy the increase in diameter is $.197\times10^{-3}$ arcsecond. The change in plate scale calculated is 1.655 parts per million.

2.3.7 Random Combination of Radial and Circumferential Force Errors at Axial and Lateral Support Locations

This is divided into two combinations of errors. Forces were applied in the radial direction and then in the circumferential direction. This simulates errors in the direction the forces are applied, producing components in other than the intended direction. The forces are random in magnitude with a Gaussian distribution with a three standard deviation value of 10 Newtons. A component of force of this magnitude would result from an error in the direction the nominal force is applied of 3°.

For radial direction errors the surface deformation was 110 nm peak to valley and 19.6 nm rms prior to correction with the active optics system. After correction the surface was .73 nm peak to valley and .082 nm rms. Figure 2-9 shows the deformation of the mirror surface due to the force errors in the radial direction. In interpreting the figures note that there is a difference between the contour intervals.

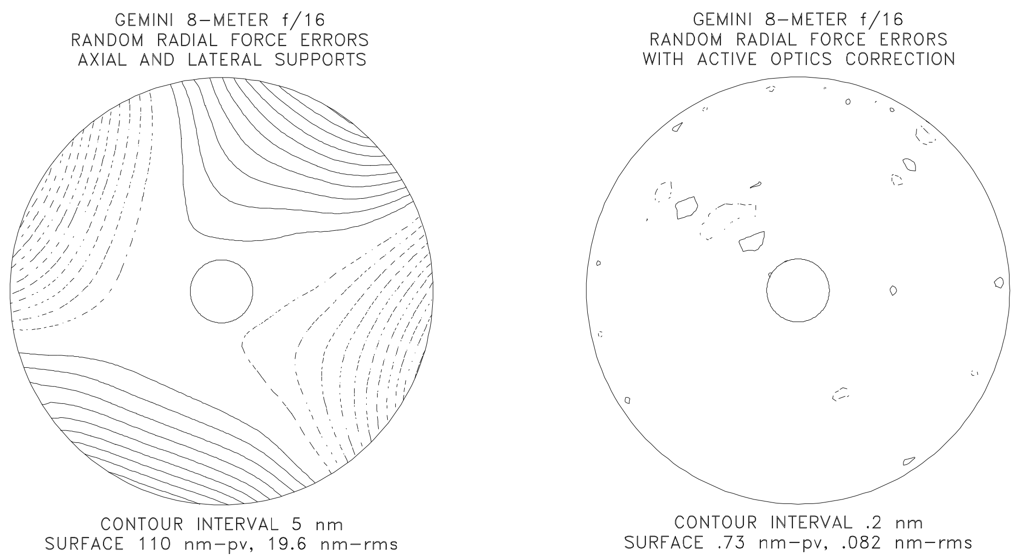

Figure 2-9: Surface Deformations from Random Radial Forces

The forces in the circumferential direction produced a surface of 43 nm peak to valley and 4.9 nm rms prior to correction with the active optics system. The active optics system improved the surface to .069 nm peak to valley and .0038 nm rms. Plots of the two deformations appear in figure 2-10. Note that the plots were made with different contour intervals.

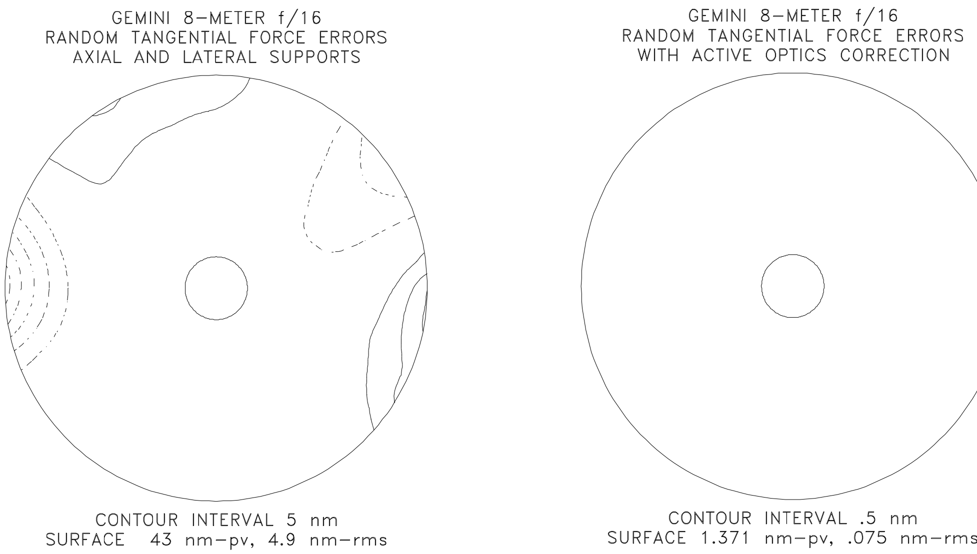

Figure 2-10: Effects of Random Circumferential Force Errors

The radial force errors produced an increase in the diameter encircling fifty percent of the energy of 35.3×10^{-6} arcsecond and an increases for 85 percent of $.217\times10^{-3}$ arcsecond. The circumferential force errors resulted in increases in the diameter encircling fifty percent of the energy of 26.8×10^{-6} arcsecond and $.159\times10^{-3}$ arcsecond for 85% encircled energy. Combining the values for the two directions in quadrature, the increase for fifty percent of the energy is 44.3×10^{-6} arcsecond and $.270\times10^{-3}$ arcsecond for 85 percent. The total change in the plate scale for the combination is .004 parts per million.

2.3.8 Normal Forces at Outer Seal Too High

Contact pressures between the air seal and the mirror must exist for the seal to function. The amount the seal is compressed will effect the magnitude of the normal force exerted on the mirror. A normal force of 1 Newton was applied at each node of the FEM over the outer air seal. There are 144 nodes over the outer seal. This translates into a loading of 5.64 Newtons per meter of circumference. This case is used to establish properties of the seal. This condition produced a surface deformation of 28 nm peak to valley and 6.9 nm rms prior to correction with the active optics system. After correction with the active optics system, the surface was improved to .92 nm peak to valley and .11 nm rms. Figure 2-11 shows the mirror surface before and after correction with the active optics system. Note the difference in contour intervals between the two plots.

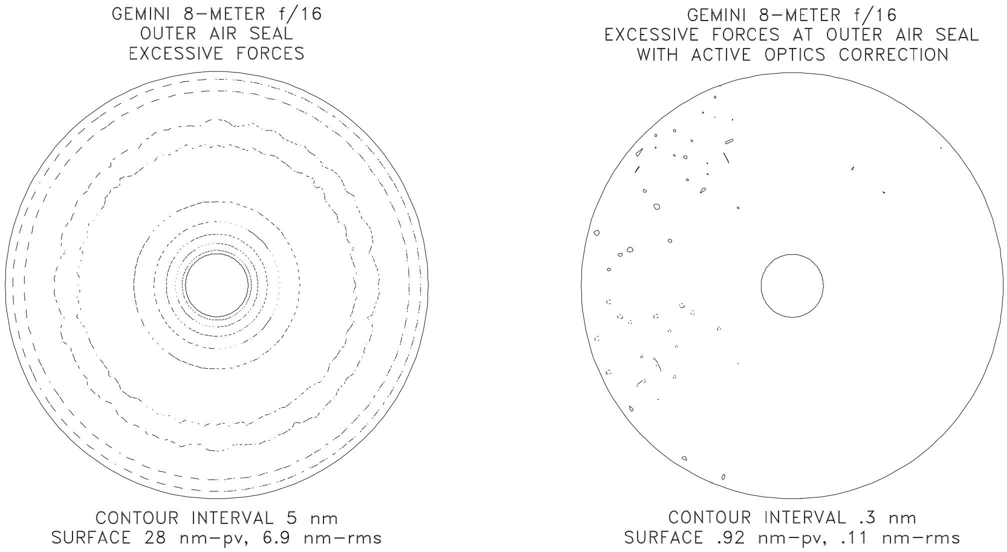

Figure 2-11: Effects of Excessive Normal Force at the Outer Air Pressure Seal

The diameter encircling fifty percent of the energy increased by 33.7×10^{-6} arcsecond. For 85 percent of the energy the diameter increased by $.188\times10^{-3}$ arcsecond. Change in plate scale is 3.41 parts per million.

2.3.9 Radial and Shear Force Errors at the Outer Seal

This combination simulates the effects of a decenter of the mirror relative to the cell. The decenter will be resisted by forces exerted by the seal. Along the direction the mirror decenters, the deflection of the seal will be in a radial direction. On the sides 90° from the direction of decenter the deflection will be in a direction tangential to the seal. The seal will have a stiffness in the radial direction different from that in the tangential direction. A component of force resisting the decenter has the form1+cosine of the position angle. The forces applied had a maximum value of 4 Newtons. This amounts to a maximum load rate of 22.56 Newton per meter. This case was analyzed to set limits on the properties of the seal in the two directions. The mirror surface was deformed by 98 nm peak to valley and 16.1 nm rms prior to active optics correction. With active optics correction, the surface deformation was .38 nm peak to valley and .037 nm rms. Figure 2-12 shows contour plots of the surface before and after correction. In interpreting the plots the difference in contour intervals should be noted.

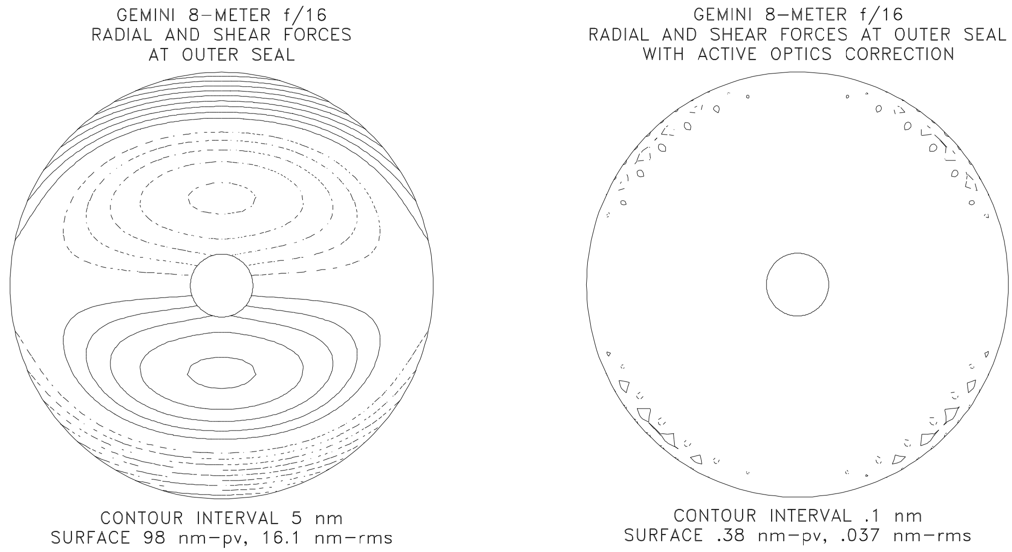

Figure 2-12: Effects of Radial and Shear Forces at the Outer Air Pressure Seal

Image degradation is 12.9×10^{-6} arcsecond for fifty percent encircled energy and 62.0×10^{-6} arcsecond for 85 percent encircled energy. The change in plate scale is 2.25×10^{-6} parts per million.

2.3.10 Normal Force at Inner Seal Too High

A normal force must be exerted by the air pressure seal on the mirror to maintain a pressure difference across the seal. Axial deflections of the seal will also change the magnitude of the normal force. At each node over the inner seal a normal force of 1 Newton was applied. There are 72 nodes over the inner seal. The diameter of the central hole is 1.2 meter. The equivalent seal loading is 19.10 Newtons per meter of circumference. This case was analyzed to establish limits on the properties of the seal. The surface that resulted from this was 150 nm peak to valley and 38 nm rms. The active optics system improved the surface to 6.7 nm peak to valley and 1.00 nm rms. Figure 2-13 shows the surface deformations. The contour intervals are different in the two plots and should be accounted for in interpreting the plots.

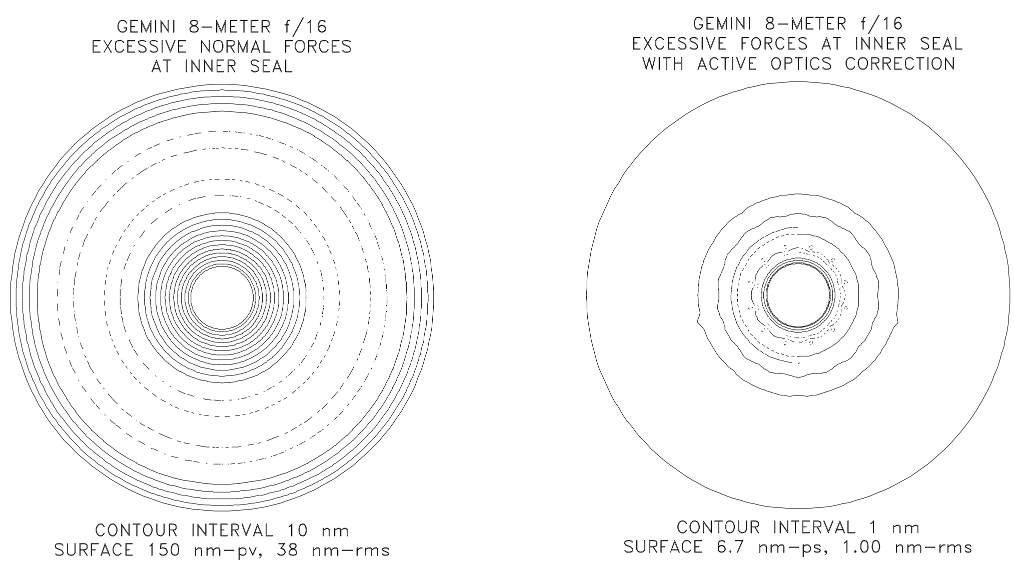

Figure 2-13: Effect of Excessive Normal Force at the Inner Air Pressure Seal

Image quality degradation was $.382\times10^{-3}$ arcsecond for fifty percent encircled energy and 2.10×10^{-3} arcsecond for 85 percent encircled energy. The change in plate scale is 2.17 parts per million.

2.3.11 Normal Force at Seals Vary as the Cosine of the Position Angle

If the mirror tilts relative to the mirror cell, the seal will be compressed more on one side than on the opposite side. The result could be a normal force higher on one side than the other. Around the circumference of the mirror the normal force will vary as the cosine of the position angle. Results are not yet available for this combination.

2.3.12 Normal Force at Seals Vary as the Cosine of Twice the Position Angle

This case simulates the effects of bending of the mirror cell. The normal force exerted on the mirror will be higher where the mirror cell deflects toward the mirror and lower where the deflection is away from the mirror. For an astigmatic shape, the normal force will have a component that varies as the cosine of twice the position angle. Results are not yet available for this combination.

2.3.13 Forces and Moments Produced by Mirror Decentration in the Y Direction

The moments and forces were combined to reflect the relative stiffness in those two modes of the actuator flexure considered at the time of the analysis. A force of 5 Newtons and a moment of 1 Newton-meter were applied at each support location. This simulates a mirror decenter of .1 mm. The force was applied in the Y direction and the moment applied about the X direction consistent with the simulated shift in mirror position. Prior to correction with the active optics system the mirror deformation resulting from these loads was 383 nm peak to valley and 73 nm rms. With active optics correction the mirror figure was improved to 1.16 nm peak to valley and .14 nm rms. Figure 2-16 contains contour plots of the mirror surface prior to and after correction with the active optics system. In interpreting the plots note there is a difference between the contour intervals in the two plots.

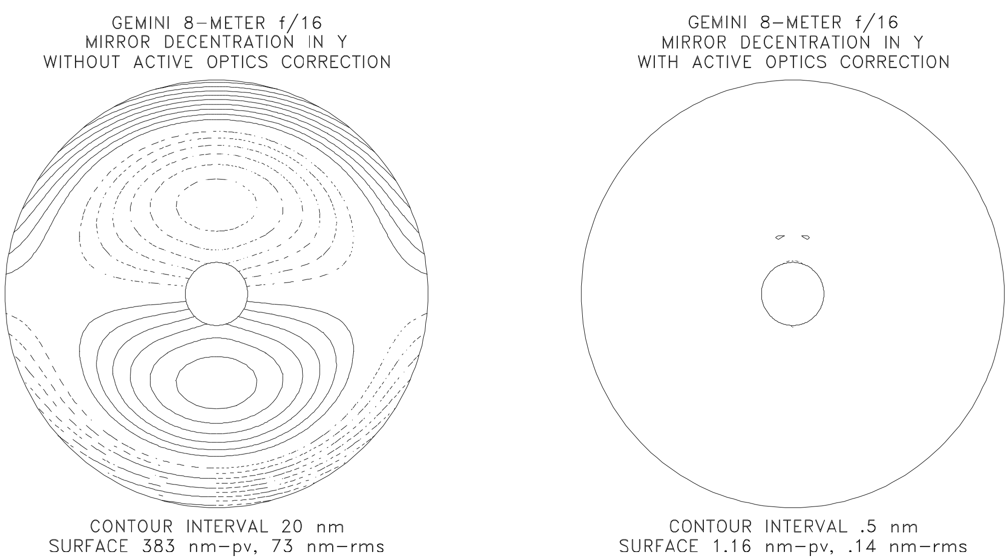

Figure 2-16: Effects of Shift in Mirror Position

The degradation in image quality after correction is an increase in the diameter encircling fifty percent of the energy of 52.0×10^{-6} arcsecond. For 85 percent encircled energy the increase is $.305\times10^{-3}$ arcsecond. The change in plate scale is 10.58×10^{-6} parts per million.

2.3.14 Random Combination of Lateral Support Force Errors

Amplitudes of force errors applied by the lateral support actuators were generated with a random number generator. This case was analyzed to assess the sensitivity of the mirror to errors in the force magnitude at the lateral supports. The errors have a Gaussian distribution with a three standard deviation value of 0.5 Newton. The resulting errors were applied in a random pattern. Figure 2-17 contains contour plots of the surface deformation without and with active optics correction. Note that the plots are generated with different contour intervals.

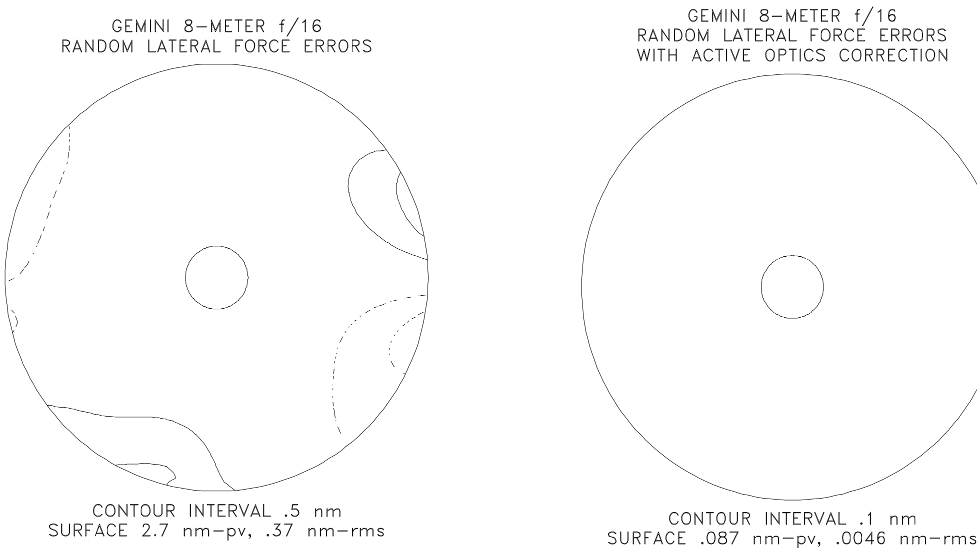

Figure 2-17: Effect of Random Lateral Force Errors

An increase of 1.32×10^{-6} arcsecond in the diameter encircling fifty percent of the energy resulted after correction with the active optics system. The diameter for 85% encircled energy increased 6.85×10^{-6} arcsecond. The plate scale changed by $.774\times10^{-6}$ parts per million.

2.3.15 Air Pressure Support Pressure Error

The print through of the axial actuators to the mirror surface is a function of the portion of the mirror's weight they must support. The air pressure support system is designed so the axia actuators support twenty percent of the mirror's weight from zenith pointing to approximately 78° zenith angle. Any deviation from this amount may produce a small amount of print through from the axial actuators to the mirror surface. This was analyzed by having the air pressure support system support 82 percent of the mirror's weight. This case was analyzed to find the sensitivity of the mirror surface to errors in regulating the pressure in the air pressure support. The mirror figure was then improved using the active optics system. The mirror figure that was achieved is 5.4 nm peak to valley and 1.0 nm rms. Figure 2-18 shows a contour plot of the mirror surface.

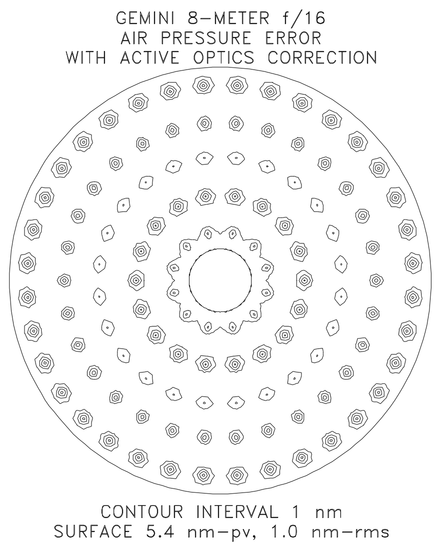

Figure 2-18: Effect of Air Pressure Errors

The increase in the diameter encircling fifty percent of the energy was $.35654 \times 10^{-3}$ arcsecond. The degradation for 85 percent encircled energy was 1.9060×10^{-3} arcsecond. The plate scale change was .232 parts per million.

Section 3
ERROR BUDGET

3.1 General Error Budget

The *Gemini System Error Budget Plan* has established an allowable image degradation value for the primary mirror and its support system. It also establishes a maximum allowable value for any change in telescope "plate scale", or effective focal length change. The error budget, as it applies to the primary mirror, is further detailed in *Summary of the Error Budget, as it Affects the Primary Mirror.* These should be consulted for a complete detailing of the total system error budget and more in-depth discussion of the errors that apply to the primary mirror and its supports.

Nine cases were identified for evaluation. These cases must satisfy the requirements given in the references above. The nine cases are the combined effects of various errors that act on the mirror in the same way. The cases are:

- Case 1: nominal support design
- Case 2: random normal force errors
- Case 3: lateral force errors
- Case 4: errors from the six zone defining system
- Case 5: orthogonal forces and moments
- Case 6: position errors
- Case 7: air pressure errors
- Case 8: air seal force errors
- Case 9: change from optics shop to telescope

Many of the cases in the error budget are the combined effects of the combinations of errors of section 2. These cases may be considered as categories of errors. For instance, orthogonal forces and moments includes all cases that produce forces in other than the intended direction or that exert moments on the mirror at the points of attachment. Descriptions of the combinations that go into the error budget are contained in section 2 of this report.

The error budget is built up by scaling the loads and deformations of the unit loads. The results are combined to obtain the total effect on the mirror surface and the resulting performance degradation. The unit loads are described in section 2. The appropriate analysis results were scaled and used to simulate a particular effect on the mirror. An example of this is the weight of the axial pads at horizon pointing. In this case, the results of analysis of uniform forces in the Y direction, part of the analysis of 2.3.13, were scaled to the maximum allowable weight of the pads. The scale factors used for simulating gravity orientation are derived from the nature of the particular effect.

3.2 Image Quality

The overall image degradation allowance for the primary mirror support system is .010 arcsecond increase in diameter for 50% encircled energy and .022 arcsecond for 85% encircled energy at a wavelength of 2.2 µm. This requirement applies in the zenith pointing orientation. Further allowance is made at other than this orientation. See the *Summary of the Error Budget, as it Affects the Primary Mirror* for a description of this allowance. The total image quality error budget allowance must be divided between several cases.

The allowable errors and the resultant image degradation are summarized in table 3-1. Also in table 3-1 is the image quality requirement for comparison to the total error calculated. Some of the categories contain more than one error. In those cases, allowable error N/A, the allowable errors will be given in the paragraphs describing those cases. The verbal descriptions indicate which error combinations of section 2 should be consulted for detailed discussion of the case.

			image degradation, arcsecond diameter			
	allowable error		zenith pointing		75° zenith angle	
category	zenith	75°	50%	85%	50%	85%
nominal support design	N/A	N/A	0.000	0.000	0.005	0.013
random normal force errors	2.0 N	2.0 N	0.004	0.010	0.004	0.010
random lateral force errors	10 N	500 N	0.000	0.000	0.000	0.000
random force errors in six zone defining system	.14 N/act	.95 N/act	0.008	0.012	0.064	0.099
orthogonal forces and moments	N/A	N/A	0.000	0.002	0.001	0.004
position errors	N/A	N/A	0.000	0.001	0.000	0.001
air pressure errors	5%	5%	0.000	0.003	0.000	0.003
air seal force errors	N/A	N/A	0.001	0.007	0.001	0.007
total, rss			0.009	0.018	0.064	0.101
requirement			0.010	0.022	0.079	0.196
allowable change, optics shop to mountain			0.003	0.010	0.030	0.100
remaining allowance for other unforeseen support errors			0.004	0.009	0.034	0.135

Table 3-1: Image Quality Degradation for Support System Errors

The last two error categories in the table are not the results of calculations. They represent error budget allowances for errors that have not been identified. They represent the remaining margin in the error budget.

3.2.1 Nominal Support Design

For the corrected surface, the enlargement of the circle for fifty percent encircled energy is .00539 arcsecond. For eighty five percent encircled energy the diameter increased .01292 arcsecond. The report *Optimization of Support Point Locations and Force Levels of the Primary Mirror Support System* should be consulted for a discussion of the nominal design performance with zenith angle.

3.2.2 Orthogonal Forces and Moments

This is the combined effect of all of the combinations of errors that produce moments on the mirror and components of force in other than the intended direction. The combinations of errors, their maximum allowable magnitudes and the effects on image quality are contained in table 3-2. Section 2 should be consulted for the individual entries in the table.

			image degradation, arcsecond diameter			
	allowable error		zenith pointing		75° zenith angle	
category	zenith	75°	50%	85%	50%	85%
random radial and tangential forces	10 N	50 N	0.0000	0.0003	0.0002	0.0013
mirror cell expansion (supports not repositioned)	100 ppm	100 ppm	0.0001	0.0003	0.0001	0.0003
random axial support angle errors	10 mrad	20 mrad	0.0003	0.0017	0.0005	0.0034
other random axial support moment errors	3 N-m	5 N-m	0.0001	0.0008	0.0002	0.0013
mirror decentration in Y direction	.1 mm	.5 mm	0.0000	0.0002	0.0001	0.0008
weight of axial pads at horizon pointing	0 N	10 N	0.0000	0.0000	0.0000	0.0000
total, rss			0.0003	0.0019	0.0006	0.0039

Table 3-2: Orthogonal Forces and Moments and Their Effects on Image Quality

3.2.3 Position Errors

The forces may be applied at locations other than nominal. In these cases there are no components of force other than in the intended direction. The forces applied are nominal in magnitude. The combinations of errors, their maximum allowable magnitudes and their effect on image quality are tabulated in table 3-3.

			image degradation, arcsecond diameter			
	allowable error		zenith pointing		75° zenith angle	
category	zenith	75°	50%	85%	50%	85%
random axial support, radial and tangential	5 mm	10 mm	0.0001	0.0005	0.0002	0.0010
mirror decenter (supports repositioned)	2 mm	2 mm	0.0000	0.0002	0.0000	0.0002
mirror cell expansion (supports repositioned)	500 ppm	500 ppm	0.0000	0.0002	0.0000	0.0002
total, rss			0.0001	0.0006	0.0002	0.0011

Table 3-3: Position Errors and Their Effects on Image Quality

The case for mirror decenter is part of the analysis of 2.3.13, where uniform moments were applied as part of the analysis.

3.2.4 Air Seal Force Errors

The air support system requires sealing the space between the mirror and the mirror cell to maintain a slight positive pressure. Seals must be employed to do this. The seals exert forces on the mirror in the performance of their function. In addition to the design forces, errors in the forces may produce unintended forces on the mirror. Forces may also result from rigid body movements of the mirror, differential thermal expansion or bending of the mirror cell. The maximum allowable errors and their effects on image quality are shown in table 3-4.

category	allowable error		image degradation, arcsecond diameter			
			zenith pointing		75° zenith angle	
	zenith	75°	50%	85%	50%	85%
outer seal symmetric radial force errors	50 N/m	50 N/m	0.0002	0.0009	0.0002	0.0009
outer seal normal force too high	25 N/m	25 N/m	0.0003	0.0017	0.0003	0.0017
inner seal normal force too high	10 N/m	10N/m	0.0012	0.0065	0.0012	0.0065
outer seal friction from decenter	5 N/m	20 N/m	0.0000	0.0000	0.0000	0.0001
total, rss			0.0012	0.0067	0.0012	0.0068

Table 3-4: Air Seal Force Errors and Their Effect on Image Quality

3.3 Plate Scale

Requirements also exist for controlling the change in "plate scale", or effective focal length for the telescope and for the primary mirror assembly. The total allowable change in plate scale for the telescope is 100 parts per million (ppm). The allowance for the primary mirror is 70 parts per million. 40 ppm is allowed for the primary mirror support system. The allowance for the support system must be divided up amongst the various error cases. The allowance for each case and the resulting plate scale change are summarized in table 3-5. Some of the cases contain more than one type of error. In those cases, allowable error N/A, the allowable errors will be given in the paragraphs describing those error cases.

category	allowable error		plate scale change, ppm	
	zenith	75°	zenith	75°
nominal support design	N/A	N/A	0.0	0.0
random normal force errors	2.7 N	2.7 N	0.3	0.3
random lateral force errors	10 N	500 N	0.0	0.0
random force errors in six zone defining system	.1 N/act	1.1 N/act	0.0	0.0
orthogonal forces and moments	N/A	N/A	2.4	2.4
position errors	N/A	N/A	2.1	2.1
air pressure errors	5%	5%	0.0	0.0
air seal force errors	N/A	N/A	31.4	31.4
allowance for change, optics shop to mountain	N/A	N/A	5.0	10.0
allowance for other unforeseen support errors	N/A	N/A	5.0	10.0
total, rss			32.4	34.6
requirement			40	40

Table 3-5: Plate Scale Change for Support System Errors

The last two error categories in the table are not the results of calculations. They represent error budget allowances for errors that have not been identified. They represent the remaining margin in the error budget.

3.3.1 Nominal Support Design

This case is described in 3.2.1. No change in plate scale is associated with this case.

3.3.2 Orthogonal Forces and Moments

This case is described in 3.2.2. The change in plate scale for each combination of forces, force errors and moments are tabulated in table 3-6.

	allowable error		change in plate scale, ppm	
category	zenith	75°	zenith	75°
random radial and tangential forces	10 N	50 N	0.00	0.02
mirror cell expansion (supports not reseated)	100 ppm	100 ppm	2.37	2.37
random axial support angle errors	10 mrad	20 mrad	0.03	0.07
other random axial support moment errors	3 N-m	5 N-m	0.01	0.02
mirror decentration in Y direction	.1 mm	.5 mm	0.00	0.00
weight of axial pads at horizon pointing	0 N	10 N	0.00	0.00
total, rss			2.37	2.37

Table 3-6: Orthogonal Forces and Moments and Their Effect on Plate Scale

3.3.3 Position Errors

This case is described in 3.2.3. Changes in plate scale for each combination of errors are contained in table 3-7.

	allowable error		change in plate scale, ppm	
category	zenith	75°	zenith	75°
random axial support, radial and tangential	5 mm	10 mm	0.01	0.02
mirror decenter (supports repositioned)	2 mm	2 mm	0.00	0.00
mirror cell expansion (supports repositioned)	500 ppm	500 ppm	2.07	2.07
total, rss			2.07	2.07

Table 3-7: Position Errors and Their Effects on Plate Scale

3.3.4 Air Seal Force Errors

This case is described in 3.2.4. Changes in plate scale for these cases are shown in table 3-8.

	allowable error		change in plate scale, ppm	
category	zenith	75°	zenith	75°
outer seal symmetric radial force errors	50 N/m	50 N/m	4.90	4.90
outer seal normal force too high	25 N/m	25 N/m	30.32	30.32
inner seal normal force too high	10 N/m	10 N/m	6.70	6.70
outer seal friction from decenter	5 N/m	20 N/m	0.00	0.00
total, rss			31.43	31.43

Table 3-8: Air Seal Force Errors and Thei Effect on Plate Scale